



RESEARCH ARTICLE

Biomolecular Engineering, Bioengineering, Biochemicals, Biofuels, and Food

Obtaining model parameters of drying kinetics for highly shrinkable materials without knowing the surface area *a priori*Tao Liu¹ | Shilei Yang¹ | Nan Fu¹  | Jie Xiao¹ | Aditya Putranto² |
Xiao Dong Chen¹ ¹Life Quality Engineering Interest Group, School of Chemical and Environmental Engineering, College of Chemistry, Chemical Engineering and Materials Science, Soochow University, Jiangsu Province, China²Discipline of Chemical Engineering, Monash University Malaysia, Bandar Sunway, Selangor, Malaysia

Correspondence

Xiao Dong Chen, Life Quality Engineering Interest Group, School of Chemical and Environmental Engineering, College of Chemistry, Chemical Engineering and Materials Science, Soochow University, Suzhou, Jiangsu Province 215123, China. Email: xdchen@mail.suda.edu.cn

Funding information

National Key Research and Development Program of China, Grant/Award Number: 2017YFD0400905

Abstract

Shrinkage parameters of highly shrinkable materials such as length, diameter and surface area during drying are difficult to quantify *in situ*. However, these are significant components of an accurate model. In this study, an attempt to isolate the surface area effect is reported in order to fetch the REA model (reaction engineering approach) parameters without knowing it *a priori*. Carrot cube and cabbage leaf were selected as experimental material and dried with hot air under a range of conditions. Shrinkages was calculated using an optical method which is used to qualitatively compare with that “calculated” using the current approach. By matching the experimental temperature and moisture content profiles against time after obtaining REA parameters for both samples without knowing the surface area, the surface areas can be “calculated” numerically. Surface area was found to be affected by sample temperature as well as the moisture content. Drying simulations can be well carried out when correlating the surface area against sample moisture content X and temperature T , and it provides the best accuracy in predicting data on T and X vs. time. In addition, carrot cube can shrink ideally while cabbage leaf cannot. The overall relative errors of predicted moisture content and temperature were less than 1%.

KEYWORDS

convective drying, highly shrinkable vegetables, prediction, reaction engineering approach, surface area

1 | INTRODUCTION

Drying operations usually induce material shrinkage (volume reduction) as moisture being removed. Highly shrinkable materials have shrinkages in odd and complex shapes which sometimes are impossible to describe in simple mathematical models. Of course, measuring them comprehensively and accurately *in situ* present huge challenges if at all possible. Dehydrated fruits and vegetables are highly shrinkable materials upon drying. The shrinkage of fruits and vegetables during drying occurs when the viscoelastic matrices contract into the spaces previously occupied and strengthened by water.¹ In general, changes in shape and size of the products affect their textures and transport properties.² The

shrinkage is also a significant factor that influences the drying rate predictions. Moreover, it is one of the important quality attributes of dried foods which strongly affects the preference of the consumers (appearances and more inherently the texture).

Shrinkage changes may be characterized by volume, area, diameter, length, and so forth. Since the volume measurement is more accurate and simpler than that of the surface area, the shrinkage ratio (the ratio of the volume change) has been used in most of previous studies. The liquid displacement method has been widely used to determine the volumes of food materials because of easy operation.^{3–6} Nowadays, some non-intrusive imaging techniques are used to measure shrinkage parameters yielding surface area, shape parameters and

perimeter. Gulati et al.⁶ measured and analyzed area shrinkage *in situ* during microwave drying utilizing a digital camera and ImageJ software. Changes of area, perimeter, diameter, and shape factor during drying of pineapple, mango, and banana were measured using image analysis and these parameters were related to moisture content with second order polynomials.² Mulet et al.⁷ investigated the shape changes in the drying of potato and cauliflower using image analysis and experimental measurement. Hansson et al.⁸ experimentally measured radial and tangential shrinkage of wood with an application of computed tomography (CT). Computer vision systems were successfully designed and implemented for characterizing the shrinkage of tobacco lamina and apple discs during drying.⁹ In order to determine three dimensional shrinkage information of food samples during drying, several digital cameras fixed at different positions were used to capture the non-isotropic contraction.^{10,11} For describing the overall shape of tomatoes, Jahns et al.¹² measured compactness and eccentricities estimated from the parameters like area, perimeter, different axes. In addition, image processing algorithm has also been effectively employed to quantify the area reduction during convective drying of sugar kelp.¹³ It is noted that despite these advancements extracting quantitative data to represent shrinkage for vegetables for instance remains elusive.

To accurately predict and simulate actual heat and mass transfer during food drying process, it is inevitable to take shrinkage into account.^{14,15} Although there were extensive studies conducted for shrinkage measurement, most of them were conducted at a room temperature under equilibrium conditions. Shrinkage is usually correlated only against the moisture content. *In situ* measurement of shrinkage is much more difficult and in particular, representing the surface area in mathematical terms is also difficult. It is highly desirable to possess the technical capability of establishing meaningful shrinkage data in terms of surface area.

In the current work, initially through mathematical manipulation, it is shown that under certain conditions the surface area effect can be “hidden” when wanting to obtain the drying kinetics parameters using the REA model. The REA model has already been shown to be highly effective in numerous studies previously. Upon the obtainment of the REA parameters independently from the surface area, by matching the experimental temperature–time and the moisture content–time profiles obtained in the current work, the most relevant surface area can be “calculated.” The carrot cubes and cabbage leaves were tested in the current work. It is the first time, so accurately, that one can elucidate quantitatively the trends of surface area. A pathway to accurate modeling of drying of highly shrinkable materials such as vegetables is therefore demonstrated.

2 | MATERIALS AND METHODS

2.1 | Sample preparation

Fresh carrots and cabbages used in this study were purchased from the local market. These carrots and cabbages were packed in fresh-

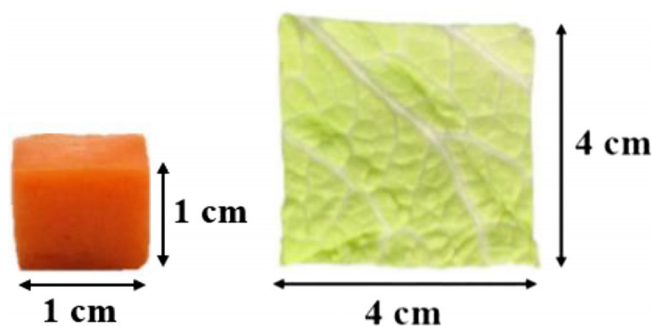


FIGURE 1 Pictures of carrot cube and cabbage leaf sample

keeping bags and stored in a fridge at 4°C for less than a week until commencing the drying experiments. Both of them were washed, respectively when needed. Carrots were peeled and cut into cubes of 1 ± 0.03 cm whereas cabbages leaves were cut into squares with side length of 4 ± 0.10 cm (see Figure 1). In each drying experiment of carrot cube and cabbage leaf, respectively, carrot cubes and cabbage leaves with similar weight (± 0.050 g) were selected as the experimental materials. Initial moisture content of the carrots and the cabbages were determined to be 11.09 ± 0.41 and 19.06 ± 0.51 kg/kg on dry basis, respectively.¹⁶

2.2 | The dryer and drying experiments

All of the chosen carrot cubes and cabbage leaves were dried in a convective dryer designed and made for this study (Nantong Dong Concept New Material Technology, Nantong, China). Schematic diagram of the dryer is displayed in Figure 2. Specific drying conditions for the carrot cubes can be found in the latest literature.¹⁷ Drying conditions for the cabbage leaves are listed in Table 1. This dryer needs 30 min to reach stable after starting. Each carrot cube and cabbage leaf was placed on the tray in the center of the drying chamber as shown in Figure 2. Weights of the carrot cube and cabbage leaf were measured using a built-in electronic balance (precision ± 0.001 g). Sample temperature was measured using thermocouples connected to a data logger (TC-08, Pico Technology, UK). The thermocouples were of K-type (accuracy $\pm 0.50^\circ\text{C}$). All the experimental data were transferred automatically to a computer. All the experiments were conducted in triplicates.

2.3 | Experimental side length and surface area

In order to capture the trends of shrinkage to allow a reasonable comparison with the theoretically obtained values. At intervals of 20 min, the carrot cubes were taken out from the drying chamber and the lengths at three directions (i.e., d_a , d_b , d_c) were quickly measured using a digital vernier caliper (1113–150, Insize Co., Ltd., China), and then it was put back into the drying chamber for next measurement. The measurement time was about 40 s. In this study, the side length of carrot cubes was taken as the geometric length:

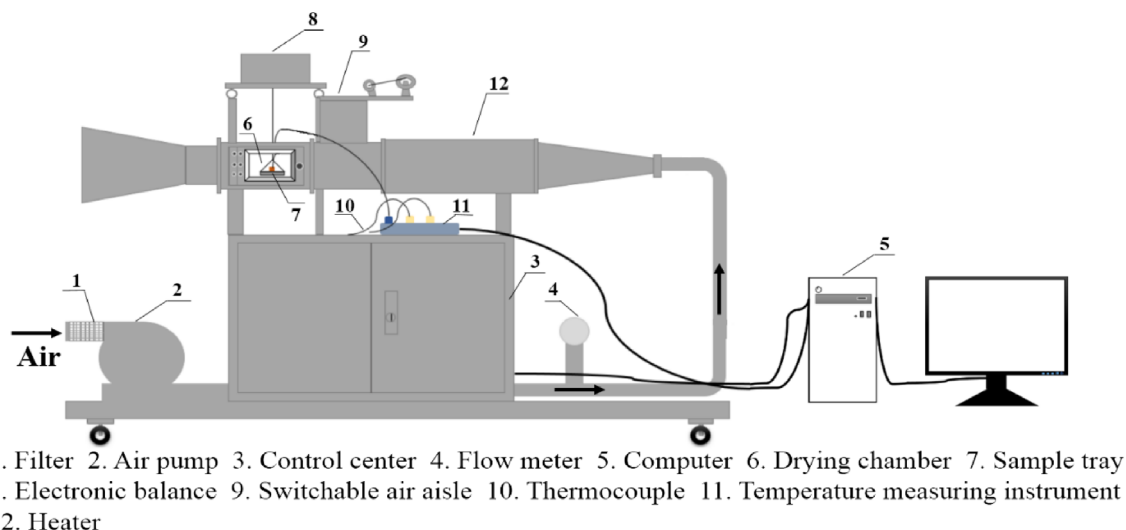


FIGURE 2 Structural diagram of self-assembly convective dryer

TABLE 1 Drying conditions for cabbage leaf

Vegetable	Initial size (cm ²)	Initial moisture content (kg/kg)	Drying air temperature (°C)	Airflow velocity (m/s)	Relative humidity (%)
Cabbage leaf	4 × 4	19.06 ± 0.51	50 ± 0.5	1.5 ± 0.2	2.42 ± 0.21
			60 ± 0.5		1.84 ± 0.24
			70 ± 0.5		0.07 ± 0.03

$$d_{\text{carrot}} = \sqrt[3]{d_a \cdot d_b \cdot d_c}. \quad (1)$$

For quantifying surface area, concave edges of the carrot cube could be taken into consideration also. Specific procedures to consider this effect is given in Figure 3. Figure 3A shows the classification strategy for the shrinkage stages of carrot cube during drying. Figure 3B demonstrates the scheme for describing and calculating the length and surface area of carrot cube during stage I and II. After removing a large amount of surface free water, where the length and width of carrot cube did not change much, and after that the shrinkage is dominated by the edge deformation. Therefore, the area of a concave surface can be properly tracked by calculating the area difference between a rectangle and four symmetrical semi-ellipses.

In contrast, owing to the soft texture of cabbage, it would be very fragile upon drying. In this study, the surface area of cabbage leaf may be determined from the following relationship¹⁸:

$$A_{\text{cabbage}} = \frac{m_{\text{cabbage}}}{SLW}, \quad (2)$$

where A_{cabbage} is the surface area of cabbage leaf (m²), m_{cabbage} is the weight of cabbage leaf (g), and SLW means the leaf weight per unit area (g/m²). Cabbage leaf is assumed to always shrink as a perfect square, thus the side length can be approximately calculated as:

$$d_{\text{cabbage}} = \sqrt{A_{\text{cabbage}}}. \quad (3)$$

2.4 | Ideal shrinkage modeling for carrot cube and cabbage leaf

As a bench mark to the new development in this work, ideal shrinkage model as a common approach in literature was also considered. In this case, the volume reduction may be solely considered as a result of water loss. For fruits and vegetables with high initial moisture contents, their shrinkage behaviors may be, at the beginning of the drying experiments, regarded as being ideal. In previous literature, it was found that the volume changes of foods such as carrot, potato, sweet potato, and apple were proportional to the volume changes of their water losses, although these literature might not be the instantaneous volume changes measured *in situ* in real time in drying.^{5,19–22}

In the current study, water loss (m_w , kg) was measured using the electronic balance *in situ* in real time, and the density of water (ρ_w , kg/m³) calculated using the established formula.^{23,24} Therefore, the volume ratio of water loss can be calculated as:

$$\frac{V_w}{V_0} = \frac{V_0 - V}{V_0}, \quad (4)$$

$$V_w = \frac{m_w}{\rho_w}, \quad (5)$$

where V_w is the volume of water loss (m³), V_0 is the initial volume of sample (m³), and V is the volume of sample at any time (m³).

(A)

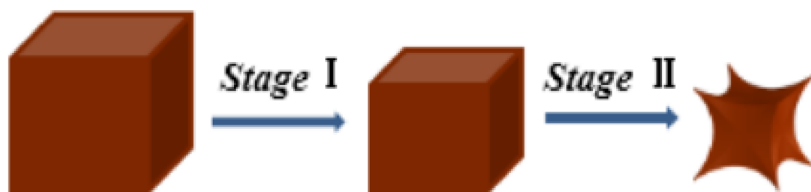
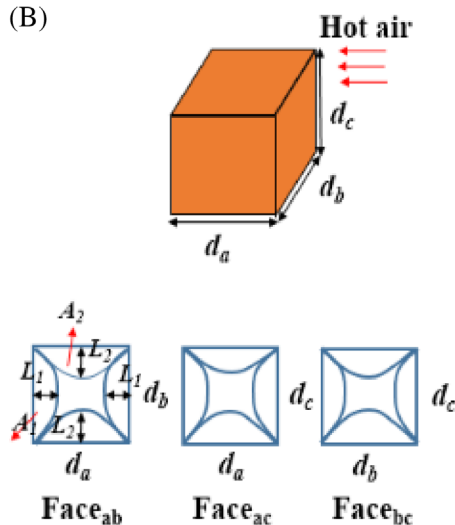


FIGURE 3 Quantification of surface area and side length of carrot cube. (A: classification of shrinkage stages; B: description of concave edges and its calculation)



(B)



Stage I:

$$d = \sqrt[3]{d_a d_b d_c}$$

$$A = 2d_a d_b + 2d_b d_c + 2d_a d_c$$

Stage II:

Example Face_{ab}

$$L_1 = \frac{d_{a(t-1)} - d_{a(t)}}{2}$$

$$L_2 = \frac{d_{b(t-1)} - d_{b(t)}}{2}$$

$$A_1 = \pi \frac{d_{b(t)}}{4} L_1$$

$$A_2 = \pi \frac{d_{a(t)}}{4} L_2$$

$$A_{ab} = d_{a(t)} d_{b(t)} - 2A_1 - 2A_2$$

$$A = 2A_{ab} + 2A_{ac} + 2A_{bc}$$

In the current study, the initial shape of carrot and cabbage was fixed as cube and square, respectively. For the ideal shrinkage calculations, the assumption that the carrot and cabbage always keep their original shapes in entire drying was necessary. Thus, the side length and surface area of carrot cube have been determined as:

$$d_{\text{carrot}} = \sqrt[3]{V_0 - V_w}, \quad (6)$$

$$A_{\text{carrot}} = 6d_{\text{carrot}}^2, \quad (7)$$

where d_{carrot} is the ideal side length of carrot cube (m), A_{carrot} is the ideal surface area of carrot cube (m²).

Although the thickness of cabbage leaf is very small (about 0.50 mm), it had to be taken into account when calculating the surface area of the cabbage leaf once the volume was known. Therefore, the side length and surface area of the cabbage leaf can be calculated as follows:

$$A_{\text{cabbage}} = \frac{V}{H}, \quad (8)$$

$$d_{\text{cabbage}} = \sqrt{A_{\text{cabbage}}}, \quad (9)$$

where H represents the thickness of cabbage leaf (m), and d_{cabbage} (m) and A_{cabbage} (m²) are the side length and surface area of cabbage leaf, respectively.

3 | MODELING THE DRYING PROCESS OF THE VEGETABLES USING THE REACTION ENGINEERING APPROACH

3.1 | A general description of the reaction engineering approach model

The lumped reaction engineering approach (L-REA) is used in this work, where an instantaneous temperature and a water content represents the material's status at any instance during drying. The drying rate of a moist material can be expressed using the following equation:

$$m_s \frac{dX}{dt} = -h_m A (\rho_{v,s} - \rho_{v,b}), \quad (10)$$

where m_s is the dry mass of the material (kg), X is the moisture content on dry basis (kg/kg), t is the drying time (s), $\rho_{v,s}$ is the vapor concentration at the material surface (kg/m³), $\rho_{v,b}$ is the vapor concentration in the drying medium (kg/m³), h_m is the mass transfer coefficient (m/s) and A is the surface area of the material (m²), respectively. Normally, the surface area A is regarded as a function of moisture content if the material shrinks during drying.^{25–28}

In Equation (10), the surface vapor concentration ($\rho_{v,s}$) can be correlated with the saturated vapor concentration of water ($\rho_{v,sat}$) using the following equation²⁹:

$$\rho_{v,s} = \exp\left(\frac{-\Delta E_v}{RT}\right) \rho_{v,sat}(T), \quad (11)$$

where ΔE_v is the additional activation energy representing the additional difficulty in removing moisture from the material after free water (J/mol) is removed. T is the temperature representative of the material (K), and R is the ideal gas law constant (J/mol/K). With Equation (11), Equation (10) can be rewritten as:

$$m_s \frac{dX}{dt} = -h_m A \left(\exp\left(\frac{-\Delta E_v}{RT}\right) \rho_{v,sat}(T) - \rho_{v,b} \right). \quad (12)$$

For small objects like droplets or thin layer materials, the material temperature T is considered to be the same as the surface temperature T_s . This is a reasonable assumption when the *Chen-Biot* number is sufficiently small.^{30,31} For samples with larger size, the uniform temperature is not so correct due to the inherent temperature difference between surface and center. In this case, a mean temperature representative of the sample may be used. Empirical formula for calculating the saturated vapor concentration under a wide range of temperature conditions (0°C to about 200°C) was summarized by Keey and expressed as³²:

$$\rho_{v,sat} = 4.844 \times 10^{-9} (T - 273.15)^4 - 1.4807 \times 10^{-7} (T - 273.15)^3 + 2.6572 \times 10^{-5} (T - 273.15)^2 - 4.8613 \times 10^{-5} (T - 273.15) + 8.342 \times 10^{-3}. \quad (13)$$

In this study, a mean or a characteristic temperature representing the whole sample is used. The mean temperature of sample material

may be expressed according to a relationship with the surface temperature and the center temperature (see Appendix A). With this mean temperature, a lumped energy balance can be written as follows:

$$mC_p \frac{dT}{dt} = hA(T_b - T) + m_s \frac{dX}{dt} \Delta H_v, \quad (14)$$

where h is the heat transfer coefficient (W/m²/K), T_b is the drying air temperature (K), and ΔH_v represents the latent heat of water vaporization (J/kg). T is the mean temperature mentioned earlier (K). The drying rate term dX/dt is negative when drying takes place. m is the mass of the material being dried (kg) and can also be expressed as:

$$m = m_s(1 + X). \quad (15)$$

C_p represents the specific heat capacity of the material (J/kg/K) and may be calculated as:

$$C_p = C_{p,s} \frac{1}{1 + X} + C_{p,w} \frac{X}{1 + X}, \quad (16)$$

where $C_{p,s}$ and $C_{p,w}$ are the specific heat capacity of solid substance and that of water (J/kg/K), respectively. The mass transfer coefficient h_m and heat transfer coefficient h can be determined using the established correlations for Sherwood number Sh and Nusselt number Nu .³³ Thus, the apparent activation energy ΔE_v is conventionally obtained by rearranging Equation (12), then one has:

$$\Delta E_v = -RT \ln \left[\frac{-\frac{m_s \frac{dX}{dt}}{h_m A} + \rho_{v,b}}{\rho_{v,sat}(T)} \right]. \quad (17)$$

It is noted that the surface area A has to be known before this additional activation energy can be obtained. Being a semi-empirical model, ΔE_v is usually found to be the mean moisture content dependent. The dependence of this additional activation energy on moisture content is found through normalization:

$$\frac{\Delta E_v}{\Delta E_{v,b}} = F(X - X_b), \quad (18)$$

where F is a function of moisture content difference ($X - X_b$), X_b is the equilibrium moisture content. $\Delta E_{v,b}$ is the equilibrium activation energy representing the maximum ΔE_v determined by the relative humidity and temperature of the drying medium (air or gas):

$$\Delta E_{v,b} = -RT_b \ln(\phi_b), \quad (19)$$

ϕ_b is the relative humidity of drying air, and T_b is the drying air temperature (K). It should be noted that the experiments for obtaining the relevant Equation (19) have to be carried out under the very dry condition, so the final moisture content involved in drying experiments is extremely small. In addition, for individual material with the same

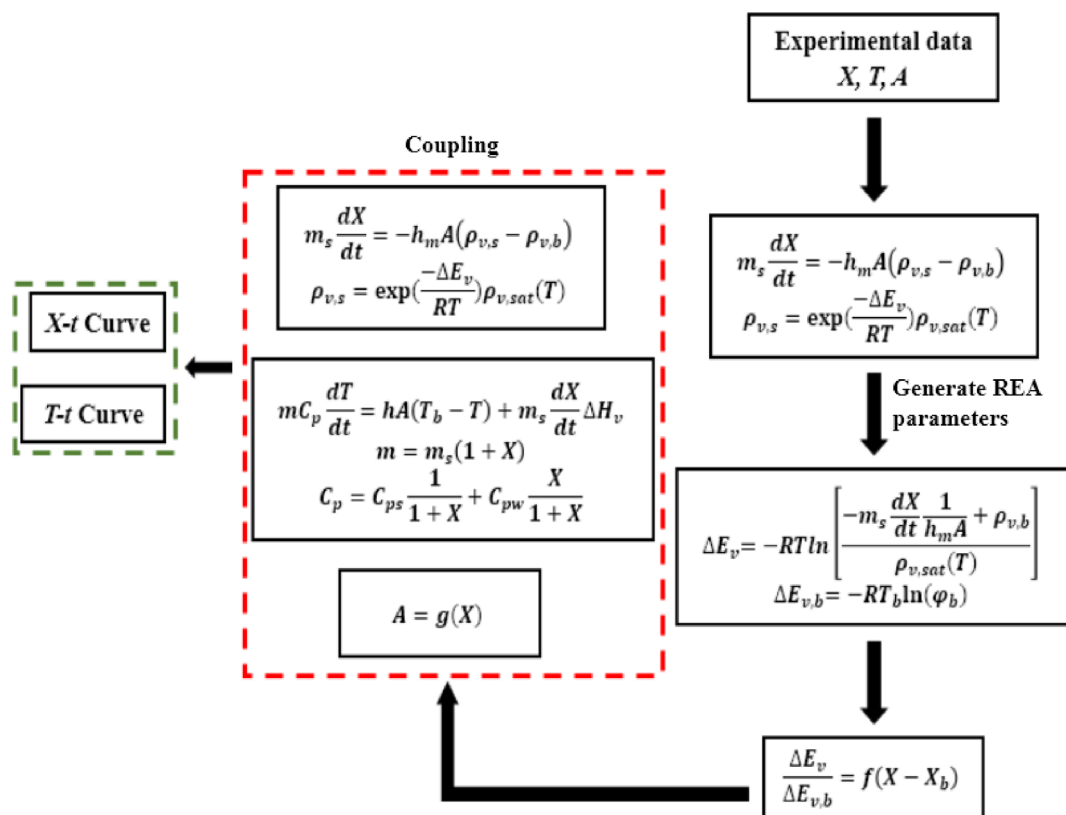


FIGURE 4 Schematic diagram of using the classical REA to predict the drying process

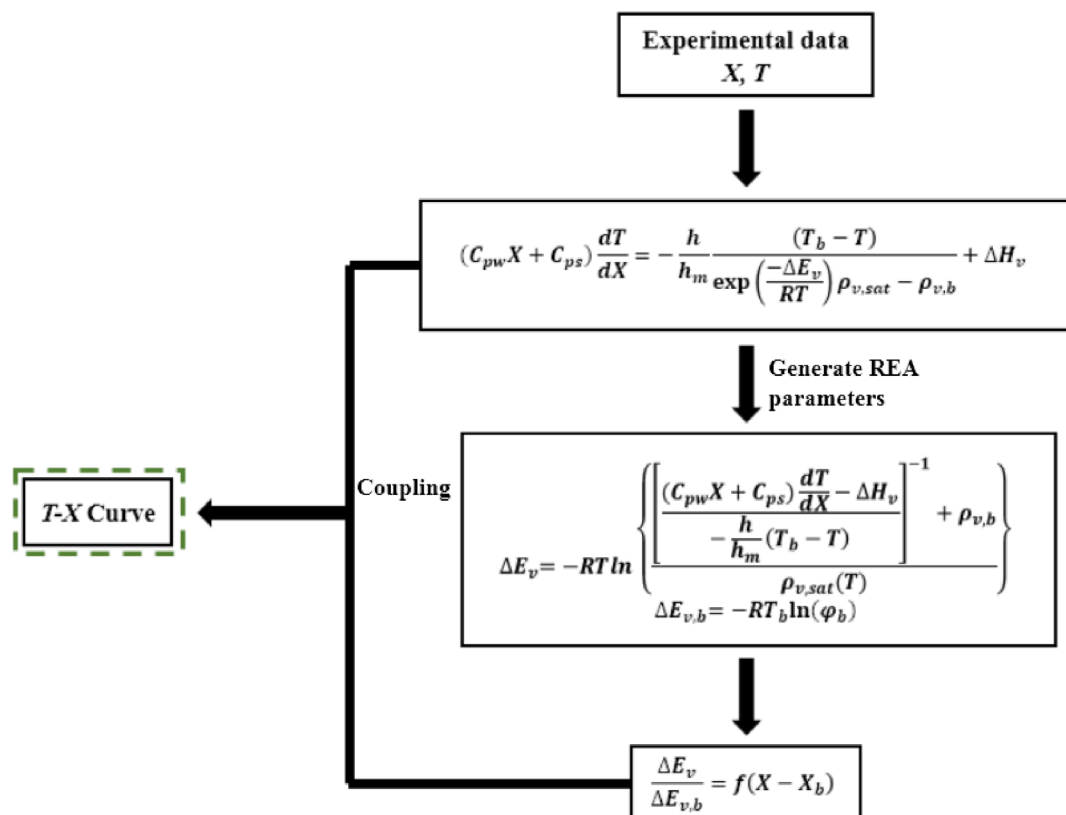


FIGURE 5 Schematic diagram of using the REA new method to predict the drying process

FIGURE 6 Framework diagram of the program for obtaining the surface area during drying

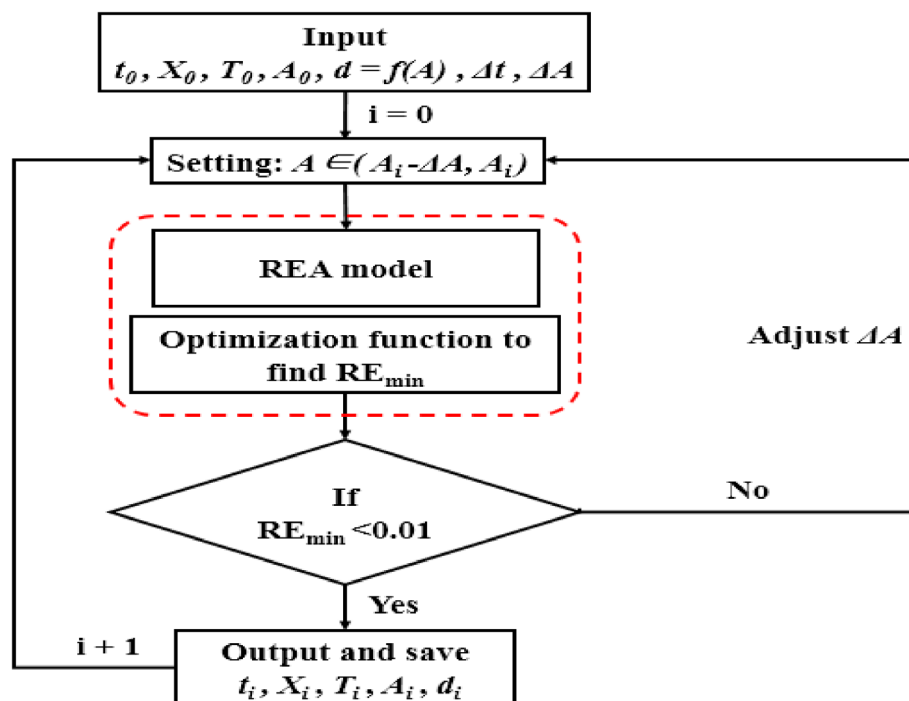
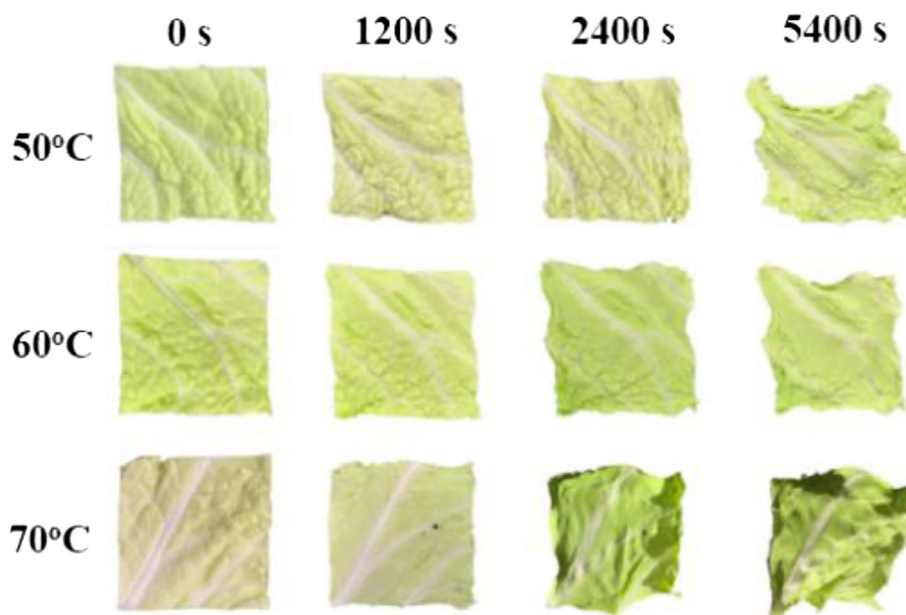


FIGURE 7 Morphology changes of cabbage leaf during drying



initial water content, the relationship described using Equation (18) was considered to be unique to the material and was insensitive to the changes of drying conditions.³⁴

3.2 | Obtaining the parameters for the REA without knowing the surface area *a priori*

As mentioned earlier, in above equations, if the surface area A and the mass transfer coefficient h_m are known, or measured by individual experiments, one reliable and accurate run of drying experiment under

the same drying air (gas) condition is sufficient for establishing Equation (18), which is the core of the REA model.

For highly shrinkable material, the shrinkage cannot be easily described in a regular way. For vegetables in general, the moisture contents are initially quite high and the products come in odd shapes. This presents challenges in accurate modeling.

In this study, it is shown, after some manipulation of the mass and energy balance in REA, the surface area effect could be “isolated” first and the REA parameters obtained independently from the temperature and moisture content records in the experiments.

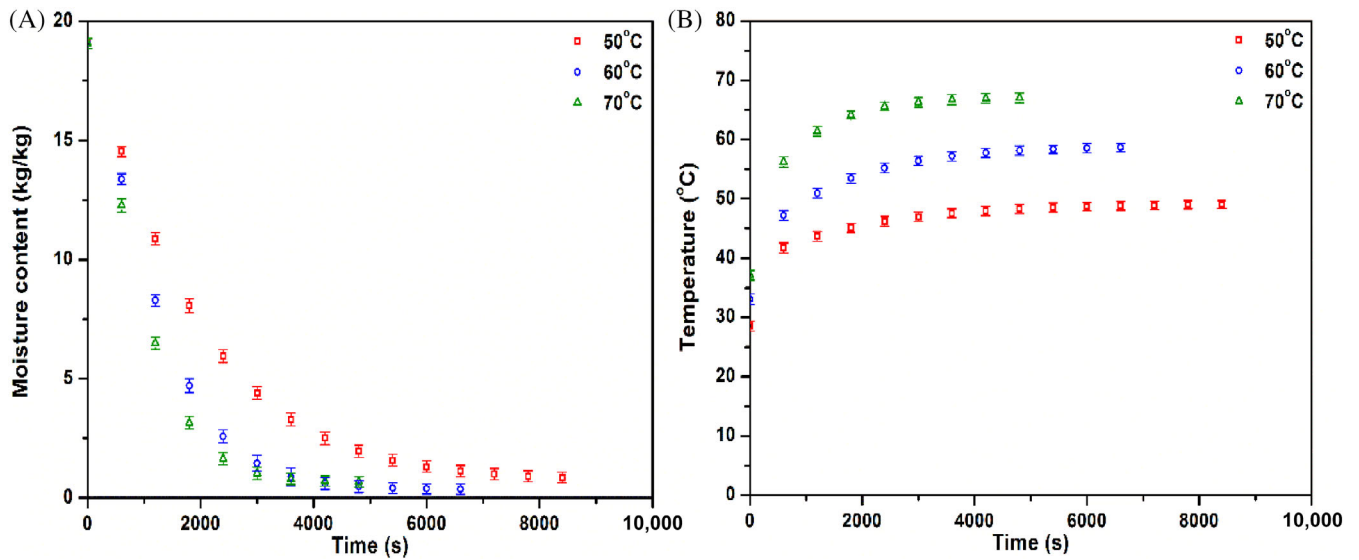


FIGURE 8 Curves of moisture content and temperature vs. time during drying of cabbage leaf

Basically, by combining Equation (15) with Equation (16), the lumped energy balance shown in Equation (14) can be rewritten as:

$$m_s(1+X)\left(C_{p,w}\frac{X}{1+X}+C_{p,s}\frac{1}{1+X}\right)\frac{dT}{dt}=hA(T_b-T)+m_s\frac{dX}{dt}\Delta H_v, \quad (20)$$

Then, on both sides, dividing with the rate of drying (Equation 12), one can obtain:

$$(C_{p,w}X+C_{p,s})\frac{dT}{dX}=-\left(\frac{h}{h_m}\right)\frac{(T_b-T)}{\exp\left(\frac{-\Delta E_v}{RT}\right)\rho_{v,sat}(T)-\rho_{v,b}}+\Delta H_v, \quad (21)$$

$$\Delta E_v=-RT\ln\left\{\frac{\left[\frac{(C_{p,w}X+C_{p,s})\frac{dT}{dX}-\Delta H_v}{-\left(\frac{h}{h_m}\right)(T_b-T)}\right]^{-1}+\rho_{v,b}}{\rho_{v,sat}(T)}\right\}. \quad (22)$$

One can see that with the known records of T and X vs. drying time t , the relationship between T and X can be worked out, leading to the obtainment of the additional activation energy which is the crucial parameter for REA formulation. It can be seen that the above-described derivations leading to Equation (22) can be of a new method provided that the ratio of heat transfer coefficient to the mass transfer coefficient is known and, in particular this ratio may be independent of the transfer area A .

It is then interesting to note that, for many heat and mass transfer scenarios, this parameter h/h_m is independent of gas velocity and transfer area, and is a ratio of thermal physical properties of the drying gas determined at the film temperature T_f (the average of the sample temperature and gas temperature). For a typical sample geometry (flat plate, cube, sphere, cylinder, etc.) in the parallel flow, one can have:

$$Nu=\frac{dh}{k_f}=C(Re)^M(Pr)^N, \quad (23)$$

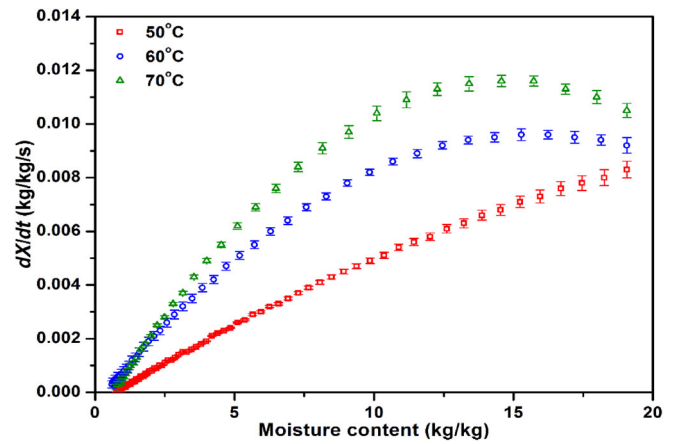


FIGURE 9 Curves of drying rate vs. moisture content during drying of cabbage leaf

$$Sh=\frac{dh_m}{D_f}=C(Re)^M(Sc)^N. \quad (24)$$

Then their ratio can be calculated as:

$$\frac{h}{h_m}=\frac{D_f}{k_f}\cdot\left(\frac{Pr}{Sc}\right)^N, \quad (25)$$

where Nu and Sh are the Nusselt number and the Sherwood number, respectively. Pr is the Prandtl number, and Sc is the Schmidt number. d is the characteristic length of the sample used for calculating the Nu , Sh , and the Reynolds number Re . k_f and D_f refer to the thermal conductivity (W/m/K) and the diffusivity (m^2/s) at film temperature T_f , respectively. Three constants C , M , and N are relevant to the sample geometry and the fluid flow circumstance. Here, C , M , and N are 0.613, 0.5, and 0.33 for carrot cube, 0.664, 0.5, and 0.33 for cabbage

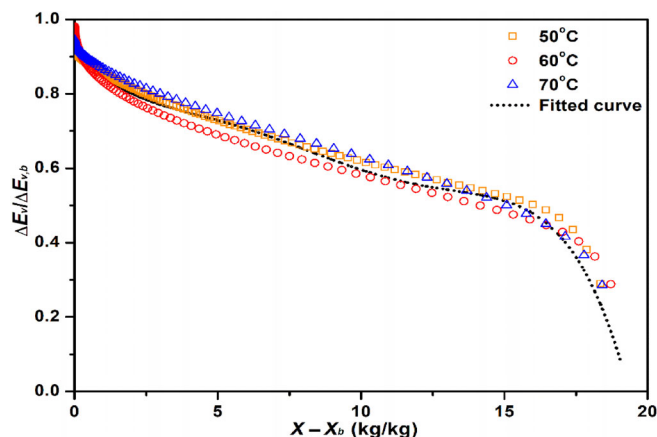


FIGURE 10 Relative activation energy curves of cabbage leaf generated by the REA new method

leaf, respectively. Noting again that the ratio of heat and mass transfer coefficients would only involve the drying gas properties. In addition to the limited usage in droplet drying because of the different heat and mass transfer correlations, this parameter can be suitably used for a wide range of sample geometries.³³

3.3 | Simulating the drying process using the parameters obtained using the conventional approach for REA which is based on Equation (17) and that based on Equation (22)

The conventional approach for REA has been widely and successfully used to simulate and predict the drying process of fruits and vegetables and other biomaterials.^{29,35–40} One of the crucial parts it is the availability of a reliable transfer surface area. For carrot cubes, the reliability and accuracy of the current approach have been confirmed in the latest investigation by our team.¹⁷ In that work, due to the more regular behavior of carrot shrinkage, the optical method for measuring size change was found reasonable. The frameworks of the conventional approach for REA and the new one for REA to simulate the drying process are shown schematically in Figures 4 and 5, respectively.

4 | THE APPROACH FOR THEORETICALLY OBTAINING THE SURFACE AREA

4.1 | Equivalence of sample dimension and surface area

It is noted, however, for a lettuce leaf, the shrinkage is difficult to capture using a simple visualization method so far. Usually for complex shapes, a geometric equivalence is applied. For example, for a sample cube with side length d_{cube} , its equivalent sphere with a radius r_{sphere} , may be worked out as:

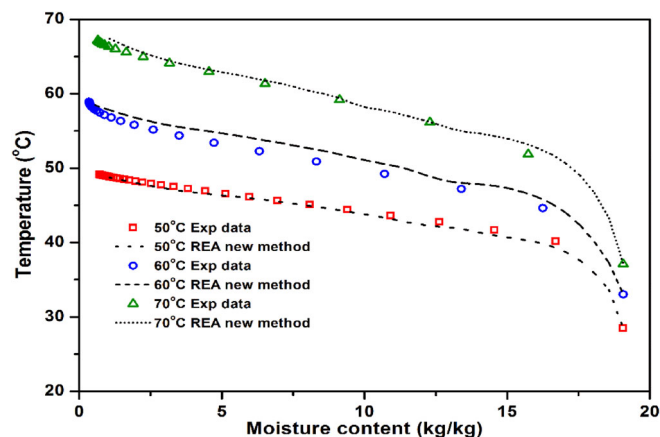


FIGURE 11 Curves of temperature vs. moisture content during drying of cabbage leaf predicted by the REA new method

$$6d_{cube}^2 = 4\pi r_{sphere}^2 \quad (26)$$

According to Equation (26), the side length of carrot cube (d_{carrot}) may be expressed with an equivalent radius:

$$d_{carrot} = \left(\frac{2}{3}\pi\right)^{\frac{1}{2}} \cdot r_{equivalent} = 1.447r_{equivalent} \quad (27)$$

Similarly, corresponding to the side length of a cabbage leaf cut into a square ($d_{cabbage}$), as another example, the surface area of the square cabbage leaf may be considered as a two-dimensional object, yielding an equivalent circle with a radius of $r_{equivalent}$:

$$d_{cabbage}^2 = \pi r_{equivalent}^2 \quad (28a)$$

or

$$d_{cabbage} = \sqrt{\pi} r_{equivalent} \quad (28b)$$

4.2 | Program for the “inverse calculation” of the surface area

In the conventional REA framework, as mentioned earlier, with the surface area (and the change of surface area) known, the REA parameters like activation energy can be worked out from one good experiment. The drying process can be nicely simulated even for other testing conditions. Indeed, if the surface area information is approximate by nature, it will affect the accuracy of the activation energy. In reality accurate shrinkage data are quite difficult to obtain. Here in this section an inverse approach for obtaining the surface area information for drying of highly shrinkable vegetables is exercised and proven beneficial. Since one can base Equation (22) to Equation (25) to evaluate the additional activation energy hence the REA model can be furnished independently without the

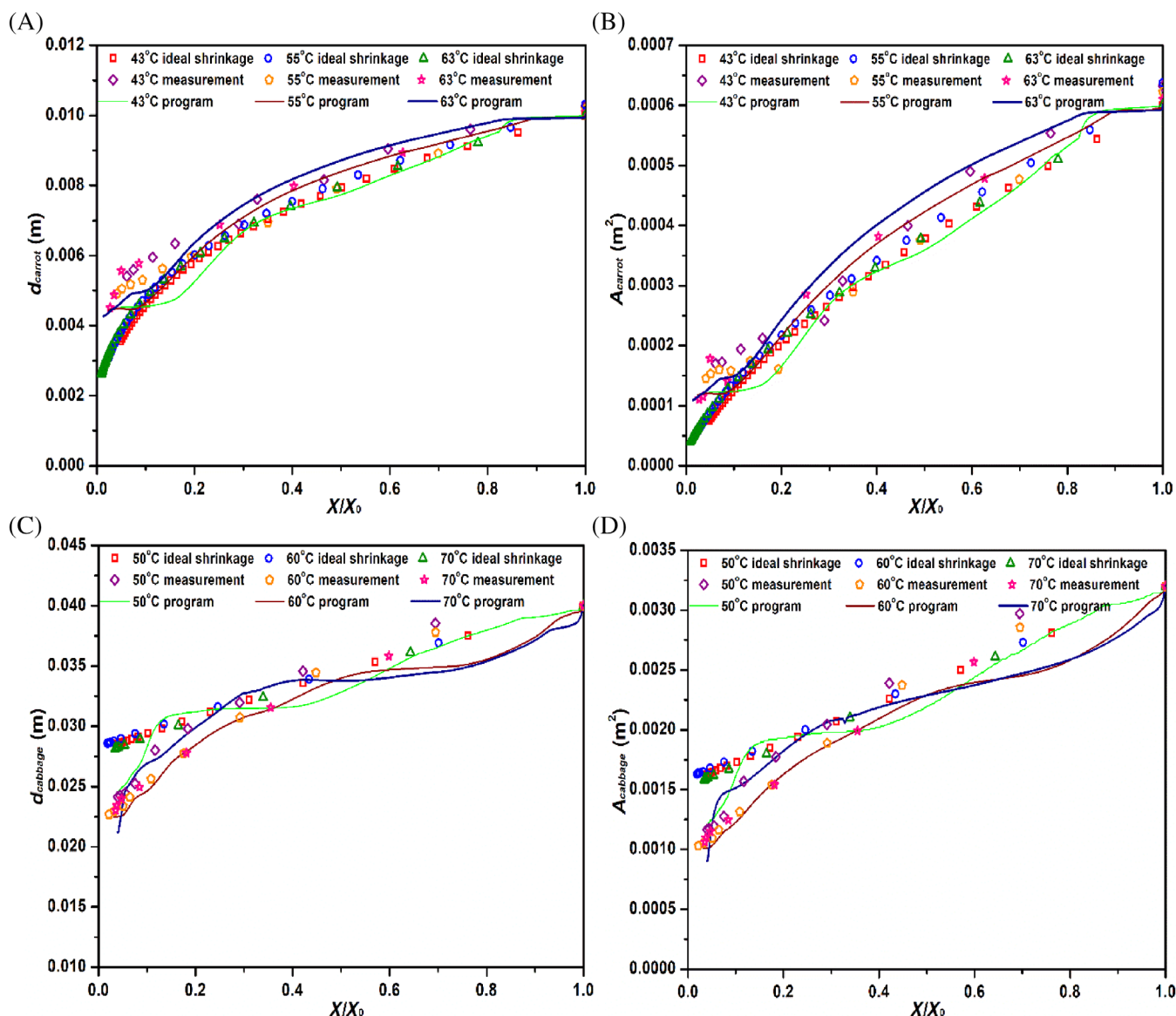


FIGURE 12 Comparison of shrinkage data obtained by the ideal shrinkage, the experimental measurement, and the program (see Figure 6). (A: carrot's side length; B: carrot's surface area; C: cabbage's side length; D: cabbage's surface area)

accurate knowledge of the surface area (or the side length). Then, with the REA model, one can “predict” the surface area (here the equivalent surface area) by running calculations of $T - t$ and $X - t$ profiles, to match as close as practical each set of the experimental $T - t$ and $X - t$ profiles.

If the initial equivalent surface area (ESA) of the material is known as A_0 , the initial equivalent side length (ESL) d_0 can be determined after the above-mentioned geometric equivalence treatment. When the drying starts, after a time step Δt , the surface area and side length are updated to A_1 and d_1 , respectively. In this way, time is increased according to the time step to find the ESL and the ESA at the corresponding time point, so that the temperature and moisture content calculated by the REA model at each time point have the highest matching with the experimental data points. The indicator of the degree of matching is the relative error (RE) between them. In this

TABLE 2 Ideal shrinkage model equations of carrot cube and cabbage leaf

Vegetables	Model equations	R^2
Carrot cube	$d = 0.01255 - 0.00822\exp(-[X/X_0]/0.84402) - 0.00193\exp(-[X/X_0]/0.07893)$	0.9921
	$A = 6d^2$	0.9986
Cabbage leaf	$d = -0.0383\exp(-[X/X_0]/2.65245) + 0.06626$	0.9935
	$A = 2d^2$	0.9978

study, when the absolute value of the relative error is less than 0.01, the relevant ESL and ESA are considered to be optimal. Therefore, in this problem, the objective function is then the relative error between

FIGURE 13 Moisture content and temperature of carrot cube predicted by coupling the ideal shrinkage model with the REA model

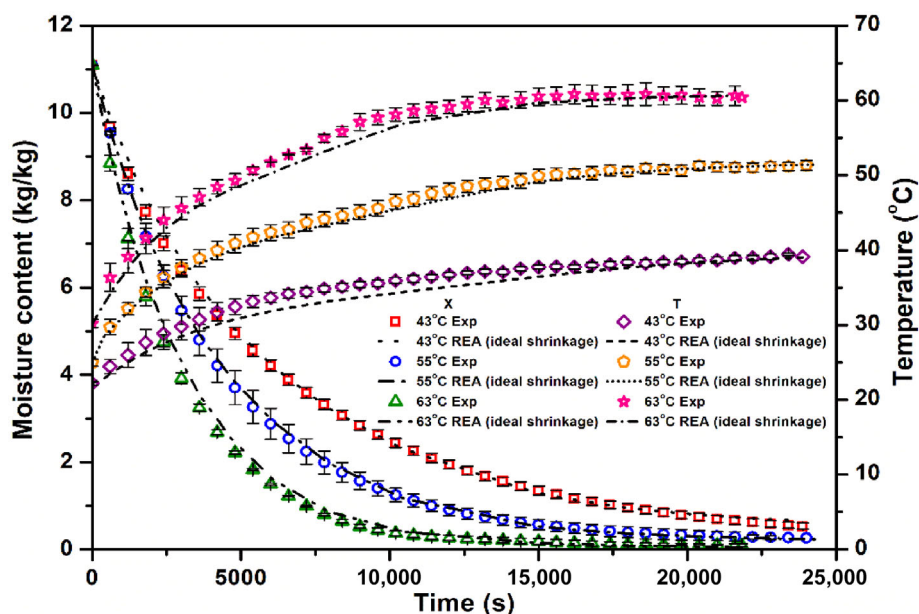
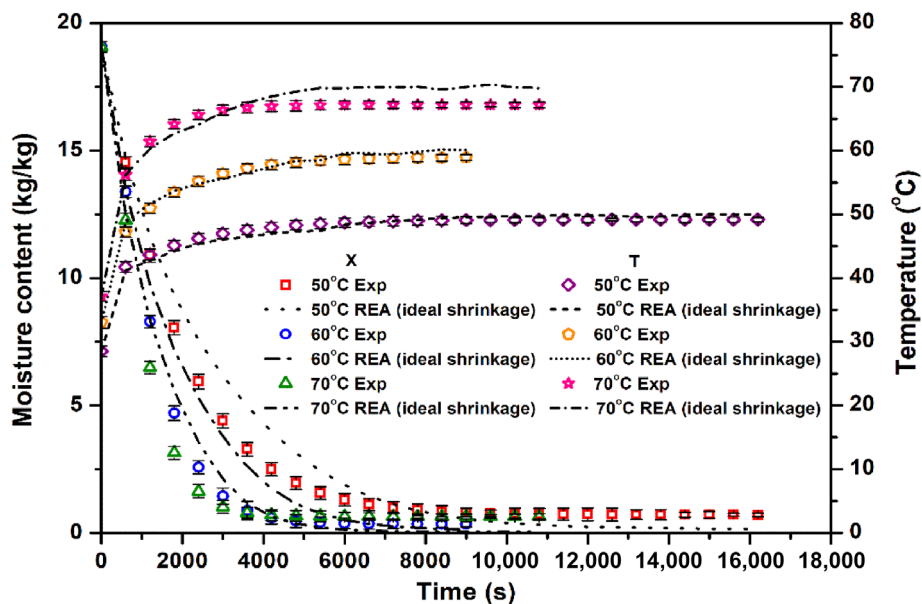


FIGURE 14 Moisture content and temperature of cabbage leaf predicted by coupling the ideal shrinkage model with the REA model



the numerically generated data from program shown in Figure 6 and the experimental data:

$$RE_{\min} = \left(\frac{|X_{\text{experiment}} - X_{\text{program}}|}{X_{\text{experiment}}} + \frac{|T_{\text{experiment}} - T_{\text{program}}|}{T_{\text{experiment}}} \right), \quad (29)$$

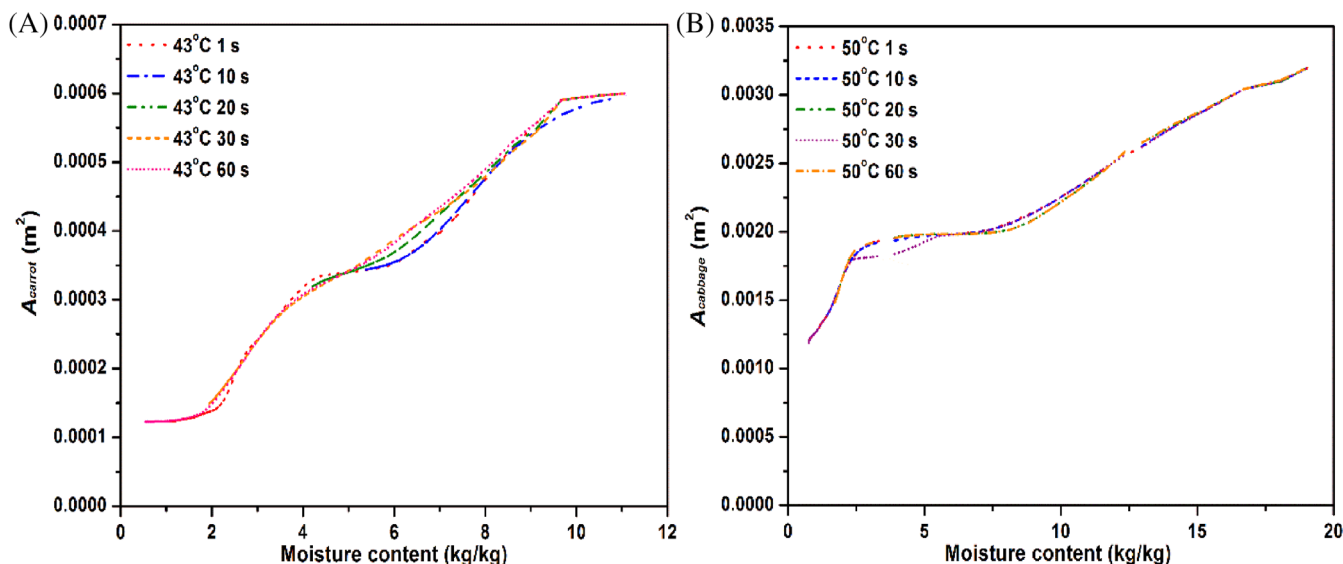
where $X_{\text{experiment}}$ and $T_{\text{experiment}}$ are the experimental data, X_{program} and T_{program} are the data generated from the program shown in Figure 6. In this study, the global optimization function “GlobalSearch” in Matlab (Matlab 2018b, MathWorks, Inc.) was employed to solve the optimization problem. “GlobalSearch” function is the most efficient way to find the global minimum on a single processor. It uses the inbuilt solver “fmincon” in Matlab, which

can be used to find the extremum of a function with several variables. The program framework for obtaining the surface area during drying is shown in Figure 6. In this program, because “GlobalSearch” function may misestimate the extremum of the objective function (too high or too low) when the gradient range of independent variable is extremely small, meanwhile, the surface area change of the vegetables was actually very little within 1 s, so the time step Δt in this study was set as 10 s which through exercises was found appropriate. This way, one can generate the ESL and the ESA vs. time. If according to the convention that a reasonable relationship between the ESL and the ESA vs. moisture content can be established, one is now equipped with a good model for the drying process.

TABLE 3 The error analysis of all calculated results

Evaluation indicators	Carrot cube				Cabbage leaf			
	IS		ES (generated from program)		IS		ES (generated from program)	
	X	T	X	T	X	T	X	T
RE	7.95%	2.19%	0.05%	0.41%	57.55%	1.80%	0.09%	0.38%
RMSE	0.12	1.09	0.01	0.14	0.23	0.31	0.03	0.19

Abbreviations: ES, equivalent shrinkage; IS, ideal shrinkage; RE, relative error; RMSE, root mean square error.

**FIGURE 15** Surface area obtained by the program under five different time steps. (A: carrot cube; B: cabbage leaf)

5 | STATISTICAL ANALYSIS

Using the inbuilt fitting toolbox in Origin (Origin 8.5pro, OriginLab, Inc.), the degree of fitting for the normalized activation energy, the degree of matching of the temperature and moisture content profiles over time with either the conventionally obtained REA (where a surface area model was known or established separately beforehand) and the REA obtained without such as a surface area model *a priori*, can be evaluated. The statistical indicators such as coefficient of determination (R^2) and root mean square error (RMSE), were used:

$$R^2 = 1 - \frac{\sum_{i=1}^n (y_{pre} - y_{exp})^2}{\sum_{i=1}^n (y_{exp} - y_{mean})^2}, \quad (30)$$

$$\text{RMSE} = \left[\frac{1}{n} \sum_{i=1}^n (y_{pre} - y_{exp})^2 \right]^{1/2}, \quad (31)$$

where y_{exp} is the experimental data (moisture content or temperature), y_{mean} is the average value of experimental data, y_{pre} is the predicted one and n is the number of data points.

6 | RESULTS AND DISCUSSION

6.1 | Changes of morphology, moisture content, and temperature during drying of cabbage leaf

The superficial morphology changes of cabbage leaf during drying were recorded by a digital camera and shown in Figure 7. Cabbage leaf deformed relatively uniformly before at least 1200 s and then gradually turns to irregular shrinkage, and the similar phenomenon was reported in the drying of carrot cube.¹⁷ Cabbage leaf drying at three temperatures shrank considerably, the edges and the surfaces became curled and uneven after drying. Generally, migration of free water has little effect on material shrinkage during food drying, while transport of intracellular and cell wall water strongly influences it.⁴¹ Therefore, the deformation of carrot cube and cabbage leaf are small and kind of uniform at the beginning of drying. Noting that the drying temperature has effect on shrinkage behaviors of carrot cube and cabbage leaf. It may be due to that structural components in the materials are temperature sensitive, especially toward higher temperatures. Previous studies also have found that much higher rate of water diffusion made material excessively dehydrated, leading to case hardening or crust.^{42,43}

As shown in Figure 8A, the moisture content of cabbage leaf reduced rapidly in the early stage of drying, afterwards, the moisture

TABLE 4 Summary of the shrinkage model's parameters

Shrinkage models	Model parameters						R^2
	a_1	a_2	a_3	a_4	a_5	/	
$d_{\text{carrot}}-X$ dependent	0.00393	0.00089	-0.0000081	-0.0000021	0	/	0.9942
$d_{\text{cabbage}}-X$ dependent	0.025	0.00042	0.00019	-0.000019	0.00000054	/	0.9795
Shrinkage models	Model parameters						R^2
	b_1	b_2	b_3	b_4	b_5	/	
$A_{\text{carrot}}-X$ dependent	0.00009	0.000047	0.0000041	-0.00000038	0	/	0.9968
$A_{\text{cabbage}}-X$ dependent	0.0012	0.000078	0.000013	-0.0000015	0.000000044	/	0.9866
Shrinkage models	Model parameters						R^2
	c_1	c_2	c_3	c_4	c_5	c_6	
$d_{\text{carrot}}-X-T$ dependent	-0.00268	0.00133	0.00024	-0.000044	-0.0000021	-0.0000052	0.9882
$d_{\text{cabbage}}-X-T$ dependent	0.80594	-0.02906	-0.02547	0.00025	0.00021	0.0005	0.9762
Shrinkage models	Model parameters						R^2
	k_1	k_2	k_3	k_4	k_5	k_6	
$A_{\text{carrot}}-X-T$ dependent	-0.00033	0.000076	0.000015	-0.0000014	-0.00000013	-0.00000007	0.9884
$A_{\text{cabbage}}-X-T$ dependent	0.08185	-0.00306	-0.00258	0.000027	0.000021	0.000052	0.9868

content decreased with much slower rate until reaching equilibrium. The trends of moisture changes at 60 and 70°C are similar, which means some of the similar drying characteristics during drying (e.g., shrinkage). Figure 8B shows that the temperature of cabbage leaf tends to be “equilibrium” before the water content. This result was similar to that reported in previous literature.⁴⁴ Under three different thermal conditions, the time for temperature of cabbage leaf to achieve stable was 0.13, 0.23, and 0.27 h earlier than that for moisture content, respectively.

The curve of drying rate of cabbage leaf vs. moisture content is plotted in Figure 9. The drying characteristics of cabbage leaf show the similarity with that of most crops.^{45–47} The initial drying rate of cabbage leaf was increased temporarily at 60 and 70°C, while that was little increase at 50°C. This may correspond to the well-known “warming up” effect.

6.2 | The REA parameters obtained using the REA new method

For carrot cubes and cabbage leaves, the relative activation energy ($\Delta E_v/\Delta E_{v,b}$) is generated from the continuous convective drying at different drying temperature conditions. Thermophysical properties of air, water and sample for model calculations are summarized in Appendix B.^{48–52} The function of relative activation energy generated using the conventional approach (i.e., Equation 17) for carrot cube has already been summarized and formulated as¹⁷:

$$\frac{\Delta E_v}{\Delta E_{v,b}} = 0.3243 \exp(-(X - X_b)/0.9332) + 2.8564 \exp(-(X - X_b)/52.3376) - 2.1726. \quad (32)$$

In the study by Yang et al.,¹⁷ it was shown that for carrot cubes, it was possible to extract the REA parameters using the new approach

(i.e., Equation 22). The model can do well once the surface area A is available (in the study of Yang et al., it was optically measured). The relative activation energy of carrot cube generated from the REA new method is expressed as¹⁷:

$$\frac{\Delta E_v}{\Delta E_{v,b}} = 0.2752 \exp(-(X - X_b)/0.4747) + 1.3822 \exp(-(X - X_b)/26.2172) - 0.7438. \quad (33)$$

Similarly, in this study, the relative activation energy of cabbage leaf generated from the REA new method is expressed as:

$$\frac{\Delta E_v}{\Delta E_{v,b}} = 0.93522 - 0.10916(X - X_b) + 0.0282(X - X_b)^2 - 0.00409(X - X_b)^3 + 2.64005 \times 10^{-4}(X - X_b)^4 - 6.17846 \times 10^{-6}(X - X_b)^5. \quad (34)$$

The coefficients of determination R^2 for Equation (32), Equation (33) and Equation (34) are 0.9913, 0.9790 and 0.9805, respectively. Figure 10 shows the relative activation energy curve ($\Delta E_v/\Delta E_{v,b}$) of cabbage leaf vs. moisture content difference ($X - X_b$). As expected, the decrease in moisture content caused the increase in relative activation energy, which indicated greater difficulty in removing water from the cabbage leaf with the extension of drying. Moreover, the relative activation energy of cabbage leaf exceeded 0.2 in the initial stage of drying, which was different from that of pure water or droplets containing different solutes. It was indicated that the free water content on the surface of cabbage leaf was finite. Using the procedure introduced in Figure 5, the relationship between moisture content and temperature during drying of carrot cube and cabbage leaf can be simulated. Yang et al.¹⁷ have successfully and accurately predicted the temperature and moisture content of carrot cube during

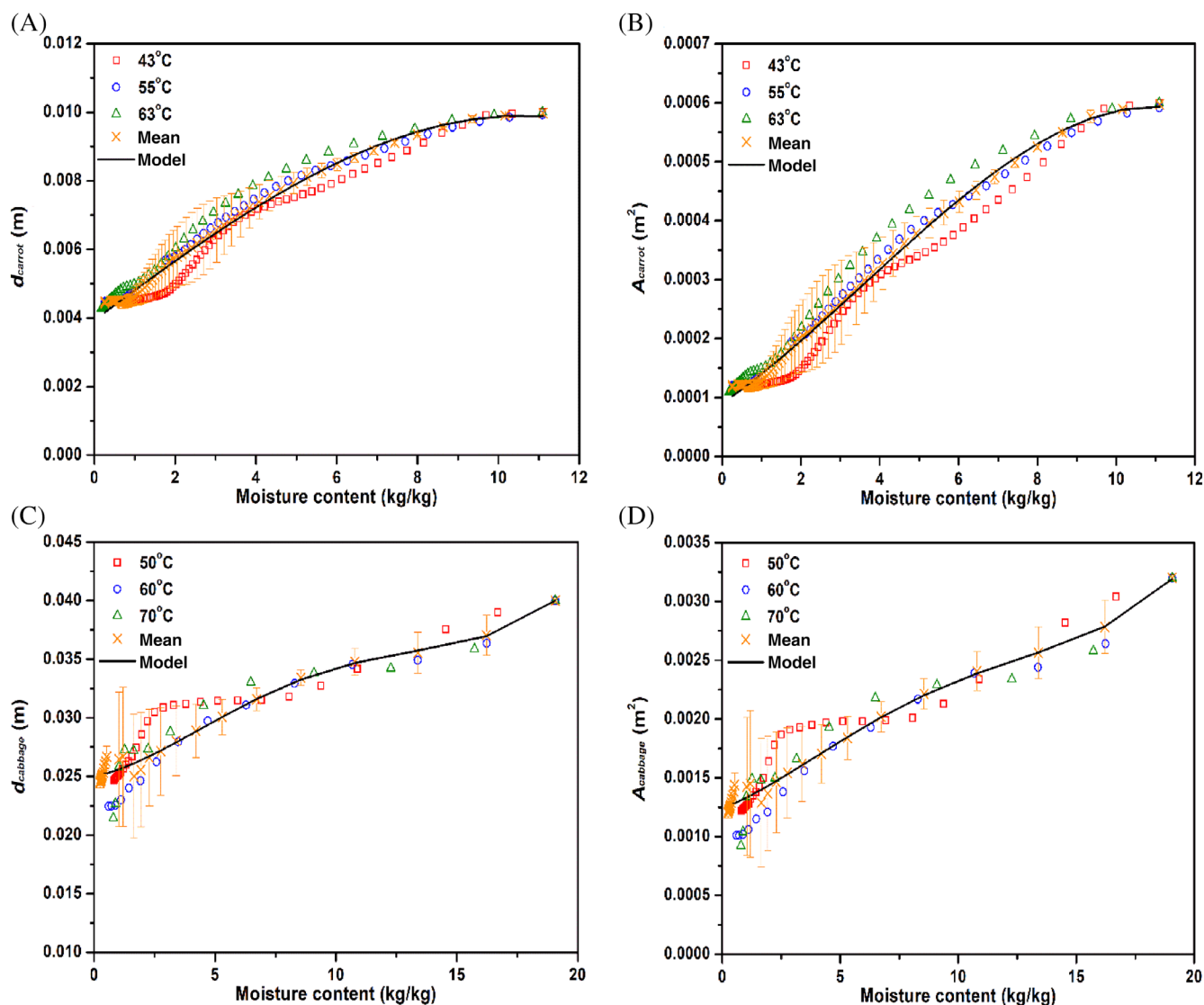


FIGURE 16 X dependent shrinkage curves of carrot cube and cabbage leaf. (A and B: carrot cube; C and D: cabbage leaf)

drying using the REA parameters obtained in the new method with the measured surface area using photographic method. For cabbage leaf, Figure 11 displays the comparison of temperature-moisture content results obtained experimentally and that matched by the trend based on the REA new method. It is seen that the calculated results of the REA new method are in good agreement with the experimental results. The overall relative error of the calculated results is 2.03%. It is noted again, this comparison does not involve the area of cabbage leaf.

6.3 | Changes of side length and surface area during drying of carrot cube and cabbage leaf calculated using the current method (new)

The shrinkage data (length and area) are generated by the three methods, that is, the experimental measurement, the ideal shrinkage

model, and the “program” shown in Figure 6, are compared. The relevant results are shown in Figure 12. Figure 12A,B represents the changes of side length and surface area during drying of carrot cube, respectively. As for cabbage leaf, the changes of side length and surface area are given in Figure 12C,D, respectively. It was found that the shrinkage behaviors of carrot cube at 55 and 63°C were more similar, while that at 43°C was slightly different. The shrinkage behavior of cabbage leaf shows more similar trend at 60 and 70°C as well, while the shrinkage behavior at 50°C is quite different. Carrot cube drying at 43°C showed a period of slowing contraction. Under the low drying temperature condition, the side length and surface area of carrot cube were smaller than that at high drying temperature condition. This may be due to the carrot surface had case hardening and crust when drying at high temperatures. This slows down further perhaps more dramatic shrinkage. The shrinkage of cabbage leaf slowed down in the middle period of drying. The shrinkage of carrot cube that is generated using the ideal shrinkage assumption, the experimentally

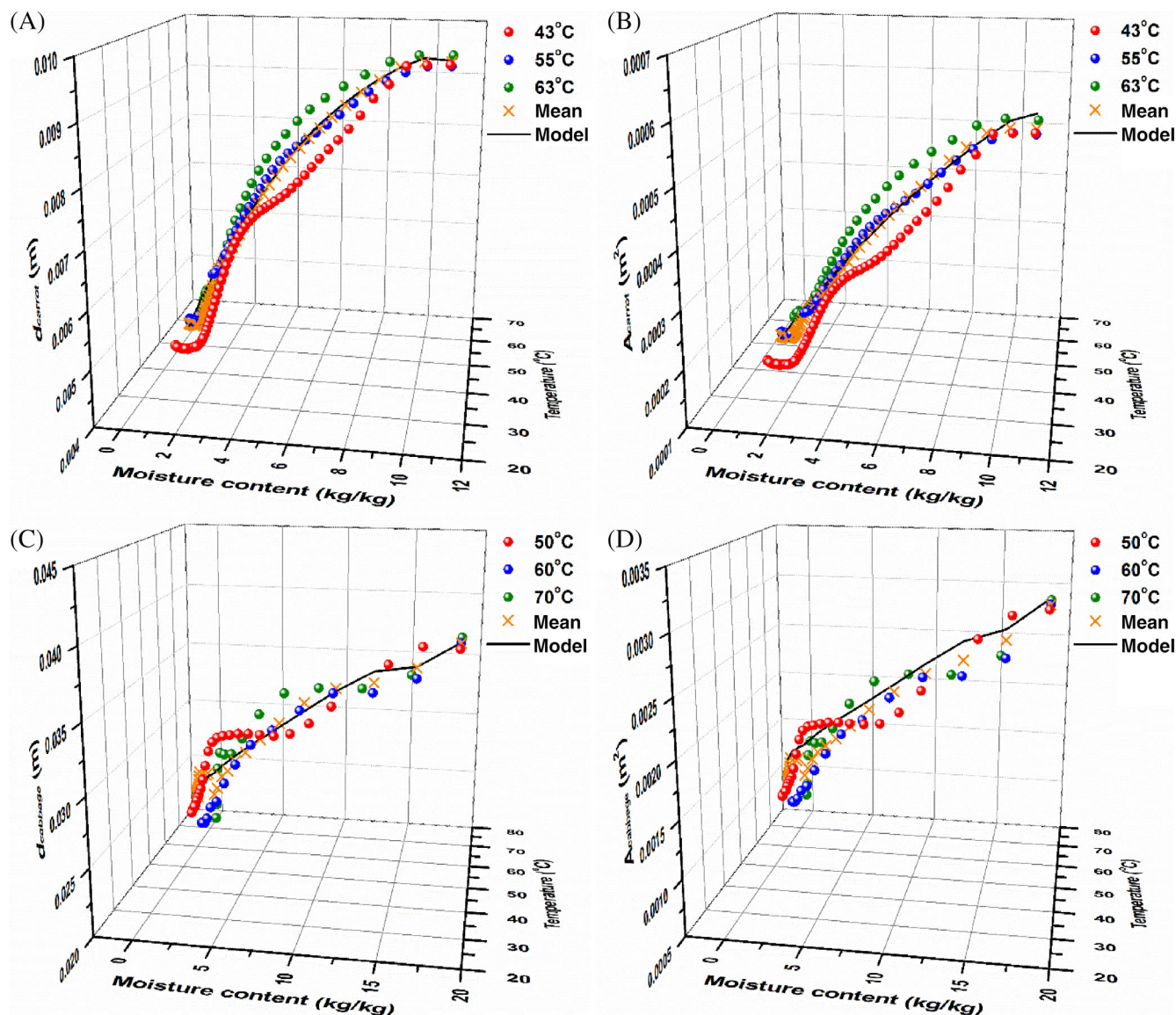


FIGURE 17 X – T dependent shrinkage curves of carrot cube and cabbage leaf. (A and B: carrot cube; C and D: cabbage leaf)

measured, and the data obtained using the new approach in this work (see Figure 6), were very close at the end of drying. However, the shrinkage trends obtained by the experimental measurement (photographic) and that calculated using the ideal shrinkage model were simpler. This is expected due to the irregular deformation and the curling of edges and the creation of more surfaces of carrot cube and cabbage leaf. The detailed processes may be complex and anisotropic.

6.4 | Modeling the drying process using the REA parameters generated by Equation (22) under the equivalent shrinkage and the ideal shrinkage

Using the inbuilt fitting toolbox in Origin, the shrinkage model equations of carrot cube and cabbage leaf are listed in Table 2. The accuracy and applicability of these ideal shrinkage models are shown in

Figures 13 and 14. As reported in previous literature, the ideal shrinkage assumption is reasonable and desirable for modeling the shrinkage of carrot sample.^{5,20} However, Figure 14 shows that the predicted moisture content of cabbage leaf does not match the experimental moisture content very well. The equivalent shrinkage data are obtained from the program shown in Figure 6. In other words, exact surface area under each drying condition can be obtained. Using the exact area vs. time or moisture content for each temperature test, one can get exact matching (see Figure C1 in Appendix C). The error analysis of all calculated results was summarized in Table 3.

6.5 | On “theoretically” measuring shrinkage data

In order to investigate the robustness and accuracy of the program (Figure 6) in this study, a sensitivity analysis of the program (see

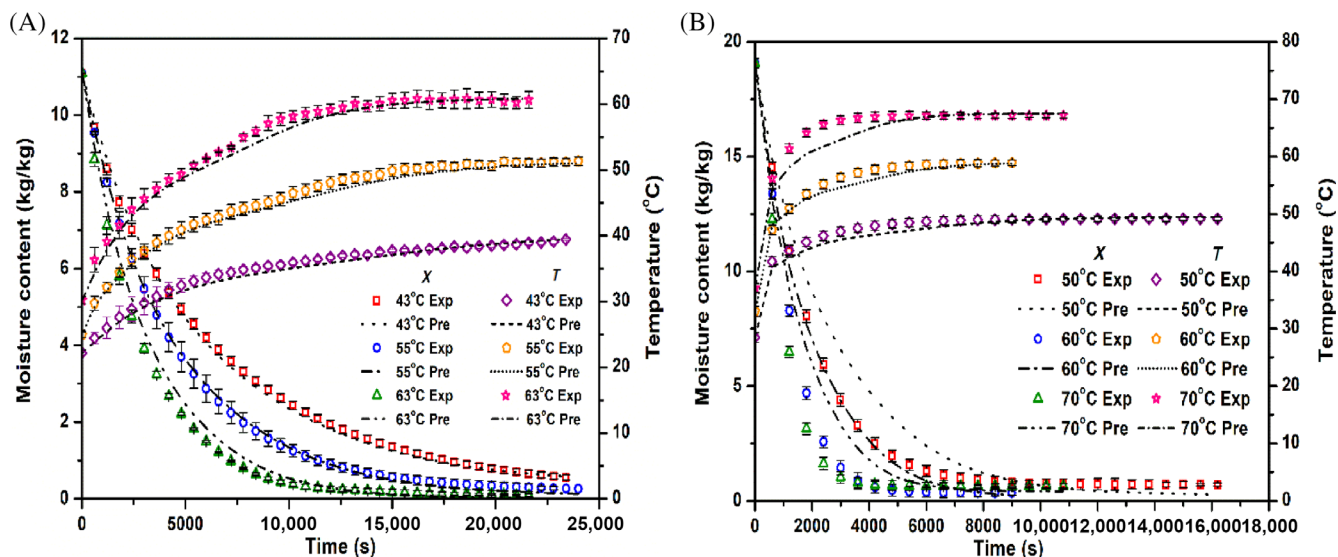


FIGURE 18 Moisture content and temperature of carrot cube and cabbage leaf predicted by coupling the X dependent shrinkage models with the REA model. (A: carrot cube; B: cabbage leaf)

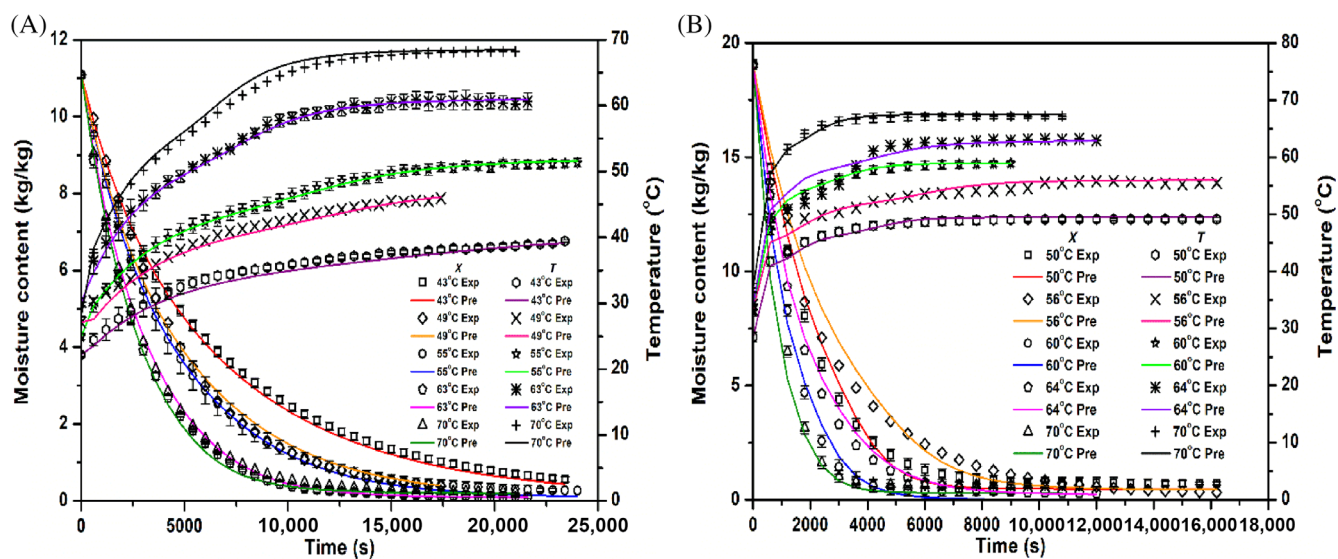


FIGURE 19 Moisture content and temperature of carrot cube and cabbage leaf predicted by coupling the $X - T$ dependent shrinkage models with the REA model. (A: carrot cube; B: cabbage leaf)

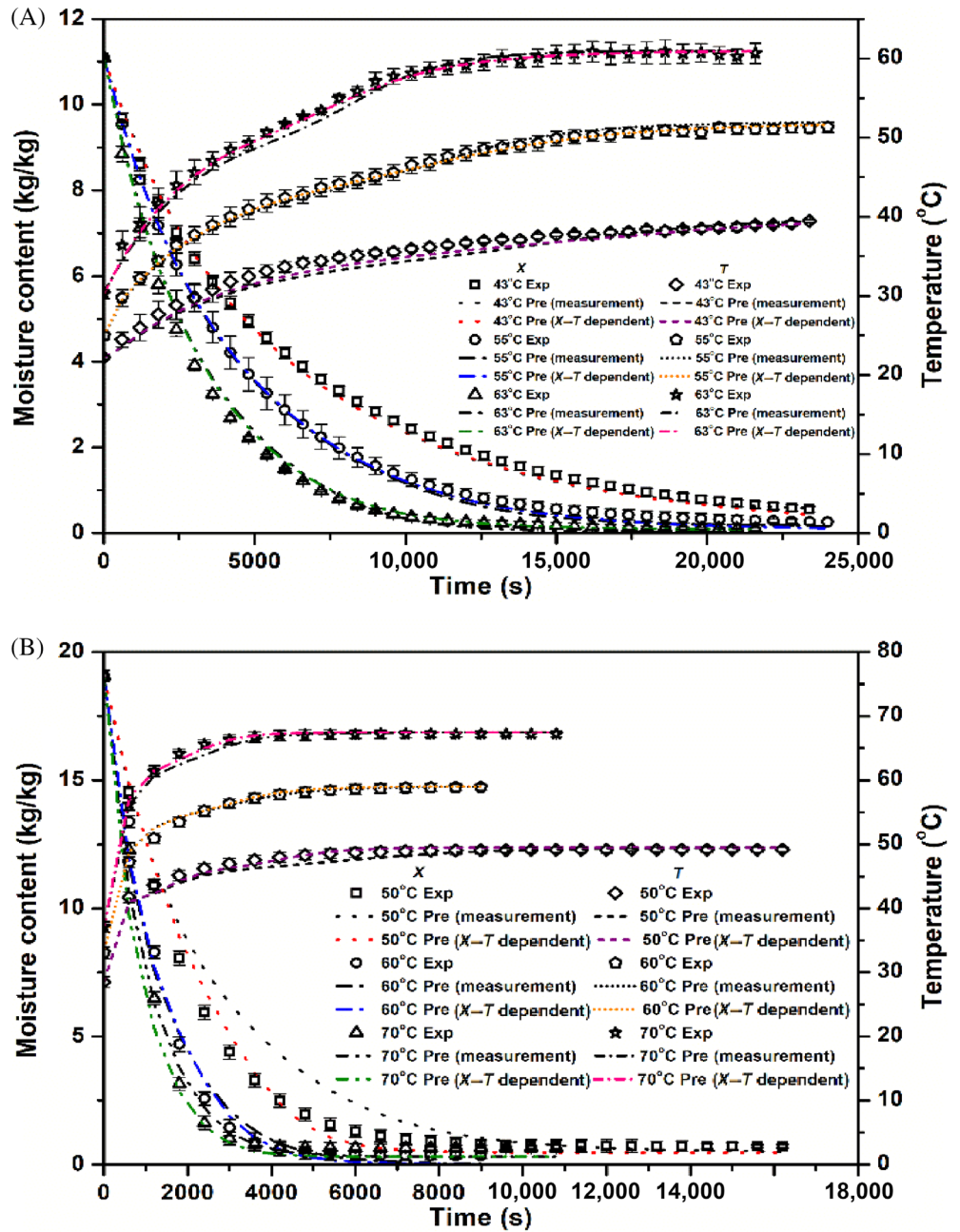
Figure 6) was carried out. The time step Δt was set as 1, 10, 20, 30, and 60 s, respectively. The program was subjected to obtain the surface area of carrot cube and cabbage leaf at 43 and 50°C, respectively. Figure 15 shows the surface area of carrot cube and cabbage leaf obtained from the program under five different time steps. It is demonstrated that the program is robust, stable, and reliable for this wide range of time steps. It has not lost the ability to capture the realistic trend. The time step 10 s was chosen for the current study according to the sensitivity analysis results.

6.6 | Modeling surface area

The shrinkage data obtained from the program in this study (see Figure 6) under three different drying air temperatures were averaged and fitted according to the conventional wisdom. The X dependent shrinkage curves of carrot cube and cabbage leaf are fitted only against moisture content X , using the following equations:

$$d = a_1 + a_2X + a_3X^2 + a_4X^3 + a_5X^4, \quad (35)$$

FIGURE 20 Moisture content and temperature of carrot cube and cabbage leaf predicted by coupling the experimentally measured shrinkage and $X - T$ dependent shrinkage models with the REA model, respectively. (A: carrot cube; B: cabbage leaf)



$$A = b_1 + b_2X + b_3X^2 + b_4X^3 + b_5X^4. \quad (36)$$

Equation (35) is for the equivalent side length and Equation (36) is for the equivalent area. In addition, the relationships between moisture content, temperature, and shrinkage can also be fitted in current study since the sample temperature is also known. The $X - T$ dependent shrinkage curves of carrot cube and cabbage leaf can be fitted against moisture content X and temperature T using the following equations:

$$d = c_1 + c_2X + c_3T + c_4X^2 + c_5T^2 + c_6X \cdot T, \quad (37)$$

$$A = k_1 + k_2X + k_3T + k_4X^2 + k_5T^2 + k_6X \cdot T. \quad (38)$$

The coefficients $a_1 - a_5$, $b_1 - b_5$, $c_1 - c_6$, $k_1 - k_6$ are the constants generated in these fitting procedures. The coefficients and the R^2 are listed in Table 4. T is the mean temperature of the sample (K). The X dependent one is not affected by sample temperature but the $X - T$ dependent one is affected by sample temperature. Figures 16 and 17 show the X dependent and the $X - T$ dependent shrinkage correlations of carrot cube and cabbage leaf, respectively. Coupling the above X dependent and $X - T$ dependent shrinkage models with the REA model generated using Equation (22), the predicted moisture content and temperature of carrot cube and cabbage leaf are presented in Figures 18 and 19. As shown in these figures, the predicted results using the $X - T$ dependent shrinkage models were better than those using the X dependent shrinkage models, and their overall root

mean square error (RMSE) for carrot cube and cabbage leaf are reduced by 23.18% and 44.45%, respectively. Moreover, the response of cabbage leaf results to the shrinkage model with the temperature effect was more obvious. As can be seen in Figure 19, the predictability of these $X - T$ dependent shrinkage models was also validated by predicting the drying process of carrot cube and cabbage leaf under other drying temperature conditions (49 and 70°C for carrot cube, 56 and 64°C for cabbage leaf). The predicted results were roughly in line with the experimental results. In this study, it is indicated that the sample temperature during drying is also an important parameter for modeling the shrinkage, in contrast to the common assumption that the shrinkage is only a function of moisture content, especially for modeling the shrinkage of leafy vegetables. For comparison, the conventional REA approach with experimentally determined surface area was used to simulate the process. Figure 20 shows that the experimentally determined surface areas for carrot cube appear to be appropriate. It is seen that the predicted result of cabbage leaf at 50°C shows worst agreement with the result generated with the $X - T$ dependent relationship. As shown in Figure 12C,D, the experimentally measured surface area for carrot cube is in good agreement with the generated one using the new approach while the data consistency of cabbage leaf is slightly worse. It is shown that different biological properties of the materials of concern influence the corresponding shrinkage behaviors.

7 | CONCLUSION

In this study, a practically useful approach was proposed based on the REA framework to ensure the high prediction accuracy of drying processes, even for highly shrinkable materials like vegetables. This approach can effectively obtain the surface area change during drying through a simple optimization scheme upon using the actual drying kinetics data and the established REA parameters (without knowing surface area *a priori*). It is demonstrated that this approach has ability to capture the shrinkage detail of the highly shrinkable vegetables (e.g., carrot and cabbage) during drying while it is known to be difficult to achieve experimentally. The surface area can then be correlated to sample moisture content only or sample moisture content and temperature both, respectively. Coupling the surface area model correlations with the REA approach, one can obtain accurate predictions of the drying process while the surface area model with the sample moisture content and temperature both as dependent parameters works the best.

ACKNOWLEDGMENT

The authors are grateful for the research fund supported and provided by the National Key Research and Development Program of China (No. 2017YFD0400905).

CONFLICT OF INTEREST

The authors declare that they have no known competing financial interests or personal relationships that could have appeared to influence the work reported in this paper.

AUTHOR CONTRIBUTIONS

Tao Liu: Data curation (equal); investigation (60%); writing – original draft (30%). **Shilei Yang:** Data curation (equal); investigation (40%); writing – original draft (10%). **Nan Fu:** Conceptualization (10%); supervision (10%); writing – review and editing (10%). **Jie Xiao:** Conceptualization (20%); supervision (20%); writing – review and editing (15%). **Aditya Putranto:** Writing – review and editing (10%). **Xiao Dong Chen:** Conceptualization (70%); funding acquisition (equal); supervision (70%); writing – original draft (25%).

DATA AVAILABILITY STATEMENT

The data that correspond to the figures are available from the corresponding author upon reasonable request.

NOMENCLATURE

A	surface area of sample (m^2)
C_p	specific heat capacity (J/kg/K)
$C_{p,s}$	specific heat capacity of dry mass (J/kg/K)
$C_{p,w}$	specific heat capacity of water (J/kg/K)
d	side length of sample (m)
D	diffusivity (m^2/s)
ΔE_v	apparent activation energy (J/mol)
$\Delta E_{v,b}$	equilibrium activation energy (J/mol)
h	heat transfer coefficient ($\text{W/m}^2/\text{K}$)
h_m	mass transfer coefficient (m/s)
ΔH_v	latent heat of water vaporization (J/kg)
k	thermal conductivity (W/m/K)
m	mass (kg)
m_s	dry mass of sample (kg)
Nu	Nusselt number (–)
Pr	Prandtl number (–)
R	ideal gas constant (8.314 J/mol/K)
φ	relative humidity (%)
Re	Reynolds number (–)
Sc	Schmidt number (–)
Sh	Sherwood number (–)
T	temperature (K)
t	drying time (s)
X	average moisture content on dry basis (kg/kg)
X_0	initial moisture content on dry basis (kg/kg)
X_b	equilibrium moisture content on dry basis (kg/kg)
ρ	density/concentration (kg/m^3)
μ	dynamic viscosity ($\text{Pa}\cdot\text{s}$)
V	volume (m^3)
F	function of relative activation energy

Subscripts

b	bulk, drying air, balance
f	film condition
s	surface/solid
0	initial state
v	vapor
w	water
sat	saturated condition

ORCID

Nan Fu  <https://orcid.org/0000-0002-4751-4645>

Xiao Dong Chen  <https://orcid.org/0000-0002-0150-0491>

REFERENCES

- Aguilera JM. Drying and dried products under the microscope. *Int J Food Sci Technol*. 2003;9(3):137-143.
- Yan Z, Sousa-Gallagher MJ, Oliveira FA. Shrinkage and porosity of banana, pineapple and mango slices during air-drying. *J Food Eng*. 2008;84(3):430-440.
- Zogzas NP, Maroulis ZB, Marinos-Kouris D. Densities, shrinkage and porosity of some vegetables during air drying. *Drying Technol*. 1994;12(7):1653-1666.
- Sjoholm I, Gekas V. Apple shrinkage upon drying. *J Food Eng*. 1995;25(1):123-130.
- Krokida MK, Maroulis ZB. Effect of drying method on shrinkage and porosity. *Drying Technol*. 1997;15(10):2441-2458.
- Gulati T, Zhu H, Datta AK. Coupled electromagnetics, multiphase transport and large deformation model for microwave drying. *Chem Eng Sci*. 2016;156:206-228.
- Mulet A, Garcia-Reverter J, Bon J, Berna A. Effect of shape on potato and cauliflower shrinkage during drying. *Drying Technol*. 2000;18(6):1201-1219.
- Hansson L, Couceiro J, Fjellner BA. Estimation of shrinkage coefficients in radial and tangential directions from CT images. *Wood Mater Sci Eng*. 2017;12(4):251-256.
- Fernandez L, Castillero C, Aguilera JM. An application of image analysis to dehydration of apple discs. *J Food Eng*. 2005;67(1-2):185-193.
- Mendiola RC, Hernandez HS, Perez JC, et al. Non-isotropic shrinkage and interfaces during convective drying of potato slabs within the frame of the systematic approach to food engineering systems (SAFES) methodology. *J Food Eng*. 2007;83(2):285-292.
- Madiouli J, Sghaier J, Orteu JJ, Robert L, Lecomte D, Sammouda H. Non-contact measurement of the shrinkage and calculation of porosity during the drying of banana. *Drying Technol*. 2011;29(12):1358-1364.
- Jahns G, Nielsen HM, Paul W. Measuring image analysis attributes and modelling fuzzy consumer aspects for tomato quality grading. *Comput Electron Agric*. 2001;31(1):17-29.
- Sappati PK, Nayak B, Walsum GP. Effect of glass transition on the shrinkage of sugar kelp (*Saccharina latissima*) during hot air convective drying. *J Food Eng*. 2017;210:50-61.
- Aprajeeta J, Gopirajah R, Anandharamakrishnan C. Shrinkage and porosity effects on heat and mass transfer during potato drying. *J Food Eng*. 2015;144:119-128.
- Pacheco-Aguirre FM, Garcia-Alvarado MA, Corona-Jimenez E, Ruiz-Espinosa H, Cortes-Zavaleta O, Ruiz-Lopez II. Drying modeling in products undergoing simultaneous size reduction and shape change: appraisal of deformation effect on water diffusivity. *J Food Eng*. 2015;164:30-39.
- AOAC. *Official Methods of Analysis*. 16th ed. Association of Official Analytical Chemists; 1995.
- Yang S, Liu T, Fu N, Xiao J, Putranto A, Chen XD. Convective drying of highly shrinkable vegetables: new method on obtaining the parameters of the reaction engineering approach (REA) framework. *J Food Eng*. 2021;305:110613.
- Pandey SK, Singh H. A simple, cost-effective method for leaf area estimation. *J Bot*. 2011;2011(2011):1-6.
- Lozano JE, Rotstein E, Urbicain MJ. Total porosity and open-pore porosity in the drying of fruits. *J Food Sci*. 1980;45(5):1403-1407.
- Lozano JE, Rotstein E, Urbicain MJ. Shrinkage, porosity and bulk density of foodstuffs at changing moisture contents. *J Food Sci*. 1983;48(5):1497-1502.
- Wang N, Brennan JG. Changes in structure, density and porosity of potato during dehydration. *J Food Eng*. 1995;24(1):61-76.
- Moreira R, Figueiredo A, Sereno A. Shrinkage of apple disks during drying by warm air convection and freeze drying. *Drying Technol*. 2000;18(1-2):279-294.
- Rahman MS, Perera CO, Chen XD, Driscoll RH, Potluri PL. Density, shrinkage and porosity of Calamari Mantle Meat during air drying in a cabinet dryer as a function of water content. *J Food Eng*. 1996;30(1-2):135-145.
- Mayor L, Sereno AM. Modelling shrinkage during convective drying of food materials: a review. *J Food Eng*. 2004;61(3):373-386.
- Mohsenin NN. *Physical Properties of Plant and Animal Materials*. Gordon and Breach Science Publishers; 1980.
- Baryeh EA. Physical properties of bambara groundnuts. *J Food Eng*. 2001;47(4):321-326.
- Al-Mahasneh MA, Rababah TM. Effect of moisture content on some physical properties of green wheat. *J Food Eng*. 2007;79(4):1467-1473.
- Barnwal P, Kadam DM, Singh KK. Influence of moisture content on physical properties of maize. *Int Agrophys*. 2012;26(3):331-334.
- Chen XD, Xie GZ. Fingerprints of the drying of particulate or thin layer food materials established using a simple reaction engineering model. *Food Bioprod Process*. 1997;75(4):213-222.
- Chen XD, Peng X. Modified Biot number in the context of air drying of small moist porous objects. *Drying Technol*. 2005;23(1-2):83-103.
- Chen XD. Air drying of food and biological materials—modified Biot and Lewis number analysis. *Drying Technol*. 2005;23(9-11):2239-2248.
- Keey RB. *Drying of Loose and Particulate Materials*. Hemisphere Publishing; 1992.
- Incropera FP, DeWitt DP. *Fundamentals of Heat and Mass Transfer*. John Wiley & Sons; 1990.
- Chen XD. The basics of a reaction engineering approach to modeling air drying of small droplets or thin layer materials. *Drying Technol*. 2008;26(6):627-639.
- Chen XD, Pirini W, Ozilgen M. The reaction engineering approach to modelling drying of thin layer of pulped kiwifruit flesh under conditions of small Biot numbers. *Chem Eng Process*. 2001;40(4):311-320.
- Putranto A, Chen XD, Webley PA. Infrared and convective drying of thin layer of polyvinyl alcohol (PVA)/glycerol/water mixture—the reaction engineering approach (REA). *Chem Eng Process*. 2010;49(4):348-357.
- Kar S, Chen XD. Modeling moisture transport across porcine skin using reaction engineering approach and examination of feasibility of the two-phase approach. *Chem Eng Commun*. 2011;198(7):847-885.
- Putranto A, Chen XD, Xiao Z, Webley PA. Modeling of high-temperature treatment of wood using the reaction engineering approach (REA). *Bioresour Technol*. 2011;102(10):6214-6220.
- Gao X, Wang J, Wang S, Li Z. Modeling of drying kinetics of green peas by reaction engineering approach. *Drying Technol*. 2016;34(4):437-442.
- Kharaghani A, Le KH, Tran TTH, Tsotsas E. Reaction engineering approach for modeling single wood particle drying at elevated air temperature. *Chem Eng Sci*. 2019;199:602-612.
- Joardder MU, Brown RJ, Kumar C, Karim MA. Effect of cell wall properties on porosity and shrinkage of dried apple. *Int J Food Prop*. 2015;18(10):2327-2337.
- Yadollahinia A, Jahangiri M. Shrinkage of potato slice during drying. *J Food Eng*. 2009;94(1):52-58.
- Gulati T, Datta AK. Mechanistic understanding of case-hardening and texture development during drying of food materials. *J Food Eng*. 2015;166:119-138.
- Phungamngoen C, Chiewchan N, Devahastin S. Effects of various pre-treatments and drying methods on *Salmonella* resistance and physical properties of cabbage. *J Food Eng*. 2013;115(2):237-244.

45. Jannot Y, Talla A, Nganhon J, Puiggali JR. Modeling of banana convective drying by the drying characteristic curve (DCC) method. *Drying Technol.* 2004;22(8):1949-1968.
46. Lahsasni S, Kouhila M, Mahrouz M, Jaouhari JT. Drying kinetics of prickly pear fruit (*Opuntia ficus indica*). *J Food Eng.* 2004;61(2): 173-179.
47. Orikasa T, Wu L, Shiina T, Tagawa A. Drying characteristics of kiwi-fruit during hot air drying. *J Food Eng.* 2008;85(2):303-308.
48. Adhikari B, Howes T, Bhandari BR, Troung V. Surface stickiness of drops of carbohydrates and organic acid solutions during convective drying: experiments and modelling. *Drying Technol.* 2003;21(5): 839-873.
49. Choi Y, Okos MR. Effects of temperature and composition on the thermal properties of foods. *Food Engineering and Process Applications*. Elsevier; 1986.
50. Wang W, Hu D, Pan Y, Niu L, Chen G. Multiphase transport modeling for freeze-drying of aqueous material frozen with prebuilt porosity. *Int J Heat Mass Transf.* 2018;122:1353-1365.
51. Poling BE, Prausnitz JM, O'connell JP. *Properties of Gases and Liquids*. McGraw-Hill Education; 2001.
52. Tzempelikos DA, Mitrakos D, Vouros AP, Baardakas AV, Filios AE, Margaritis DP. Numerical modeling of heat and mass transfer during convective drying of cylindrical quince slices. *J Food Eng.* 2015;156: 10-21.

SUPPORTING INFORMATION

Additional supporting information may be found in the online version of the article at the publisher's website.

How to cite this article: Liu T, Yang S, Fu N, Xiao J, Putranto A, Chen XD. Obtaining model parameters of drying kinetics for highly shrinkable materials without knowing the surface area *a priori*. *AIChE J.* 2022;68(7):e17728. doi:[10.1002/aic.17728](https://doi.org/10.1002/aic.17728)